



Analyzing links between simulated Laptev Sea sea ice and atmospheric conditions over adjoining landmasses using causal-effect networks

Zoé Rehder^{1,2,5}, Anne Laura Niederdrenk¹, Lars Kaleschke^{3,5}, and Lars Kutzbach⁴

¹Max Planck Institute for Meteorology, Bundesstraße 53, 20146 Hamburg, Germany

²International Max Planck Research School on Earth System Modelling, Bundesstraße 53, 20146 Hamburg, Germany

³Alfred Wegener Institute, Klußmannstr. 3d, 27570 Bremerhaven

⁴Universität Hamburg, Allende-Platz 2, 20146 Hamburg, Germany

⁵formerly at Universität Hamburg, Bundesstr. 53, 20146 Hamburg, Germany

Correspondence: Zoé Rehder (zoe.rehder@mpimet.mpg.de)

Abstract. The connection between permafrost and sea ice in the Arctic is not fully understood. As a first step, we investigate how sea ice interacts with the atmosphere over the permafrost landscape. Prior research established that Arctic-wide sea-ice loss can lead to a warming over circumpolar landmasses. However, it is still unclear which physical mechanisms drive this connection. We address this by identifying these physical mechanisms as well as local and large-scale drivers of sea-ice cover with a focus on one region with highly variable sea-ice cover and high sea-ice productivity: the Laptev Sea region. We analyze the output of coupled a ocean-sea ice-atmosphere-hydrological discharge model with two statistical methods. With the recently developed Causal Effect Networks we identify temporal links between different variables, while we use composites of high- and low-sea-ice-cover years to reveal spatial patterns and mean changes in variables.

We find that in the model local sea-ice cover is a driven rather than a driving variable. Springtime melt of sea ice in the Laptev Sea is mainly controlled by atmospheric large-scale circulation, mediated through meridional wind speed and ice export. During refreeze in fall thermodynamic variables and feedback mechanisms are important - sea-ice cover is interconnected with air temperature, thermal radiation and specific humidity. Though low sea-ice cover leads to an enhanced southward transport of heat and moisture throughout summer, links from sea-ice cover to the atmosphere over land are weak, and both sea ice in the Laptev Sea and the atmospheric conditions over the adjacent landmasses are mainly controlled by common external drivers.

1 Introduction - Laptev sea ice and permafrost

Even though sea ice and permafrost are both highly vulnerable to climate change, the mechanisms behind their interaction and its strength compared to common drivers remain unclear. To address these gaps and because this interaction is very likely mediated through the atmosphere, we explore links between the atmosphere over land and sea ice and identify local and large-scale drivers of sea-ice cover.

Though the precise physical mechanisms have not been studied, we know from prior research that sea ice can influence the atmosphere over land: Lawrence et al. (2008) found a connection between rapid sea-ice loss and temperatures on land, and Vaks

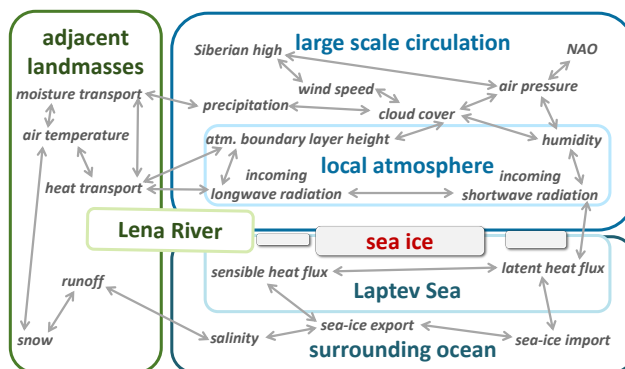


Figure 1. The regional climate system divided into general components (Laptev Sea, local atmosphere, adjacent land), which are embedded in the global climate system (surrounding ocean, atmospheric large-scale circulation) and interact with each other through a range of mechanisms including feedback loops; explanatory links indicated by grey arrows. All model variables used in the following analysis listed in grey.

et al. (2020) connected permafrost stability with the state of sea ice during climate states of the past. Under current climate, covariance of temperature and sea ice has also been found by Parmentier et al. (2015). In their analysis of satellite observations near-surface air temperature over land and sea-ice variability co-vary throughout many parts of the Arctic. They conclude, that local changes in the energy budget and ensuing temperature variations are the main mediator of a causal link from sea-ice decline to increased methane emissions. Ogi et al. (2016) investigated links between observed sea-level air pressure, two-meter air temperature and sea-ice extent in Hudson Bay and the Arctic Ocean. In contrast to Parmentier et al. (2015), they associated variability in both sea-ice cover and air temperature over the adjacent land with larger-scale atmospheric circulation fields.

We want to complete this picture by putting more emphasize on the processes responsible for the connection and disentangle causes and consequences of numerous variables interacting with sea ice. Sea ice has a strong impact on the energy balance of the ocean surface, giving rise to several feedback mechanisms, such as lapse-rate feedback (Pithan et al., 2014), water-vapour feedback (Francis and Hunter, 2007) or ice-albedo feedback, which has been identified as a major control on Arctic temperatures (Deser et al., 2000; Graversen et al., 2014). These interconnections all contribute to a strong seasonality and interannual variability of sea ice, especially in the marginal seas of the Arctic Ocean (Deser et al., 2000). Because different processes might overlay each other when looking at the Arctic as a whole, we focus on one region where we expect a comparably strong connection of sea ice and the adjacent land: The Laptev Sea is one of the key contributors to net sea-ice production in the Arctic (Bauer et al., 2013; Bareiss and Görden, 2005) and shows large year-to-year variability (Haas and Eicken, 2001) (Fig. 2). To identify the main processes between sea ice and the atmosphere over permafrost, we need to include as many variables as possible in our analysis (for an overview of all included variables, see Fig. 1). Because observations are sparse in space and time and not available for all relevant variables, we use model output. The big advantage of such a model over observational studies is that we can analyze a very large range of variables in a physically consistent system and in high resolution, both, spatially and temporally. We use forcing from the time period of 1950 to 1989. In this period and in the Laptev Sea, we do

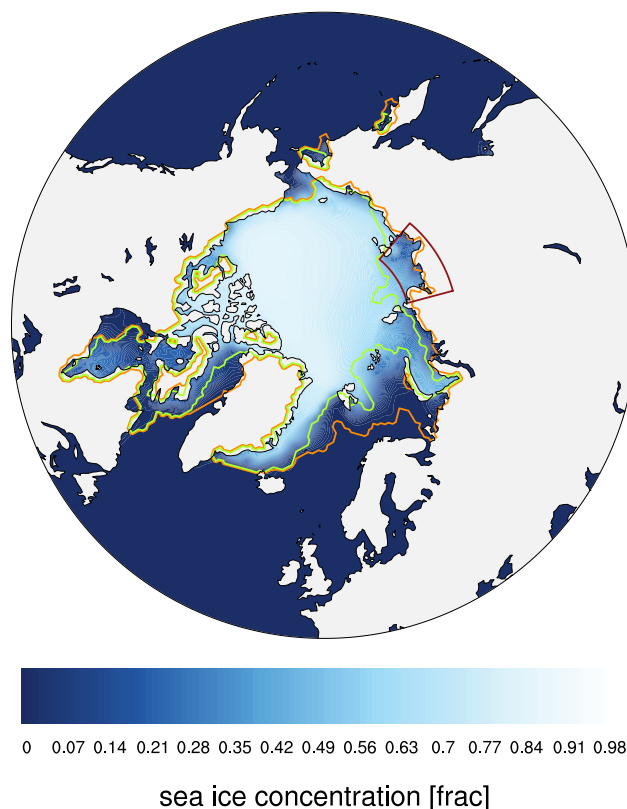


Figure 2. July monthly-mean sea-ice concentration taken from the model described above. Red box indicates Laptev Sea region and area over which one-dimensional time series of sea-ice cover are created. The contour lines show in green the minimum and in orange the maximum sea ice cover. Note, that all of the ocean in the red box might be either ice-covered or ice-free and that the Laptev Sea is one of the areas in the model with the highest variability in monthly July sea-ice cover.

not yet observe a general downward trend of sea ice. We run the model repetitively to improve statistical power. On the thus obtained 160 years of model output we employ two statistical methods. The first is called causal-effect networks, a recently developed method (Runge et al., 2012, 2014, 2015), which has been successfully applied by (Kretschmer et al., 2016) to analyze Arctic drivers of midlatitude winter circulation. This method allows us to a) identify the important links in an unbiased way and b) differentiate whether two variables are either subject to a common external forcing or which variable is forcing the other. Building on the results from the causal-effect networks, we group model-years with exceptionally high and low sea-ice cover. These composites reveal spatial patterns and mean changes in variables, allowing us to gain a deeper physical understanding.

In the following, we start with introducing the causal-effect networks and the composite analysis. Then, we analyze the impact of sea-ice cover on the atmosphere over land as well as the drivers of sea-ice cover during the onset of the melting season and during refreeze. Finally, we put our results in the wider context.

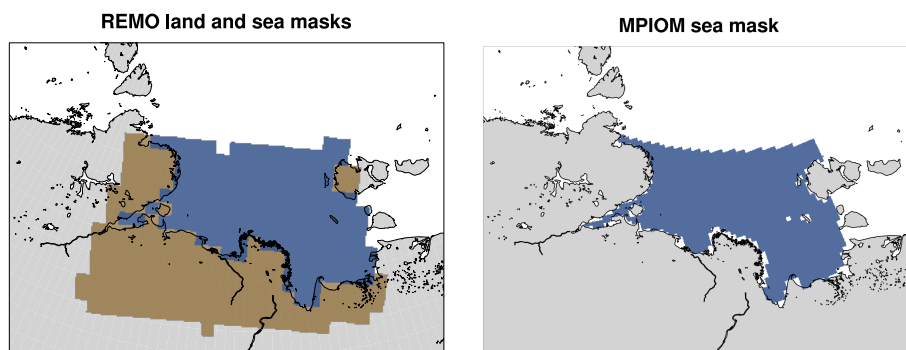


Figure 3. Model grid cells used in the analysis. Blue marks grid cells used for ocean variables, brown signifies land grid cells used to produce one-dimensional time series. MPIOM output is only available over water. REMO output was reduced either over land, over water or over both jointly. Colored areas lie between 105°E - 140°E and 70°N - 77°N.

2 Methods

In order to understand links between Laptev sea ice and regional climatic conditions, we analyze the output of a regionally
55 coupled ocean-sea ice-atmosphere-hydrological discharge model with two complementary methods. The model consists of the
global ocean-sea ice model MPIOM (Jungclaus et al., 2013) coupled to the regional atmosphere model REMO (Jacob and
Podzun, 1997; Jacob, 2001), covering most of the northern hemisphere. The atmosphere model has a horizontal resolution of
approximately 55 km and 27 vertical levels. In the global ocean model, the grid poles are located over North America and
Russia leading to a horizontal resolution of up to 5 km within the Arctic Ocean. The model has 40 vertical levels with varying
60 depth. The regional atmosphere model and the ocean model in the uncoupled domain are forced with model output from
the global model MPIOM/ECHAM5 for the time period 1950 - 1989 and the model was run repetitively. Details on the model
set-up can be found in Sein et al. (2015); Niederdrenk et al. (2016) and on the experimental design in Niederdrenk et al. (2016).

For our analysis, we use 160 years of model output in total. This output does not show a drift in sea-ice cover in the Laptev
Sea (see Fig. 4) as sea-ice decline accelerated only in the nineties. These model simulations have been validated against
65 observations by Niederdrenk et al. (2013) and show a realistic mean Arctic climate for this time period. Thus, we can use them
to examine underlying links between climate and Laptev Sea sea ice assuming no or only little disturbance through model drift
or anthropogenic forcing. Sea-ice cover is the quantity we use to represent sea ice in our analysis, since we expect that sea-ice
cover has a larger impact on atmosphere-ocean exchange processes than e.g. sea-ice volume. Sea ice covers the Laptev Sea
completely during winter, and most variability can be observed during the summer months (see Fig. 2). We, therefore, focus
70 on the summer season to understand what influences sea-ice cover and what is influenced by sea-ice cover.

As a first method we use causal-effect networks, implemented in the Python package TiGraMITe (Runge et al., 2012, 2014,
2015). Causal-effect networks determine how a perturbation moves through a set of one-dimensional time series. Each time
series represents one variable, for example precipitation, and the temporal path of the perturbation is considered as a causal link.
The procedure to find links and gauge their strength is divided into two steps. In the first, preliminary drivers of perturbations in



75 each time series are found using partial correlations. In a second step, these preliminary drivers are used to re-evaluate the link
strength between each pair of time series by applying multiple linear regression. Since a causal link implies that a perturbation
is observed in the driver before it is observed in the driven time series, the multiple linear regression is applied repeatedly while
shifting the time series against each other until the time lag between them reaches a predefined maximum. The results of all
multiple linear regressions are then summarized in a causal regression matrix of dimension (N, N, τ_m) where N is the number
80 of time series we use and τ_m is the maximum time lag. Values in this matrix range from zero to one and are similar to a partial
correlation coefficient. The threshold when a link is considered significant was set to 0.2, such that in our networks links that
are roughly two standard deviations stronger than the mean link between all time series are considered as significant. If we find
a lagged link between two time series, we call it "causal". We also consider "contemporary" links, where the time lag is zero.
For these links, it is not possible to determine the direction of information flow.

85 To get a complete picture, we select all variables given in Fig.1. We spatially reduce the data by either computing averages
or sums over the Laptev region. If the variable has a "per-area"-unit, we weight the sum using the grid-cell area. Most of
the variables are non-directional scalar fields, but for the vector fields, such as wind, we split them into their zonal (positive
sign: West to East) and meridional (positive sign: South to North) component and reduce them separately. There are not only
horizontal but also vertical fluxes. These we either integrate vertically over the atmosphere, or only consider surface fluxes
90 from atmosphere to land, ocean or ice. Lastly, for ice transport, we compute the gross import and export out of and into the
Laptev area. The boxes for the atmosphere and ocean model are given in Fig. 3.

To resolve effects on different scales, we analyze both monthly and daily means. When analyzing monthly-mean time series,
we consider the past year ($\tau_m = 12$ months) as maximal time lag, while we allow a lag of one week ($\tau_m = 7$ days) in the daily
set-up. We look at drivers of variables during June - September when vegetation is photosynthesizing and sea-ice cover is low
95 and variable. We additionally investigate what drives sea-ice evolution. To do so, we investigate the phases of strong changes
in early ice melt and ice refreeze in spring and fall. While the Laptev Sea is still completely ice-covered in March in most
years, sea-ice cover starts declining in April in most years, so we consider the month April, May, June for ice melt. Starting
in September, ice cover grows from its minimum extent to a nearly complete cover in November. Consequently, for the ice
refreeze we focus on the month of September, October and November. Since our goal is to connect land and sea-ice cover, we
100 only consider the atmosphere over landmasses adjacent to the Laptev Sea (see brown area in Fig. 3) for the summer period
(June - September). In contrast, for early ice melt (April - June) and ice refreeze (September - November), we also want to
understand what drives sea ice. So for these two cases, we look at the atmosphere over land and ocean together (entire shaded
area in Fig. 3).

With causal-effect networks, we can disentangle temporal relationships. To also understand spatial patterns and quantify
105 dependencies, we extend our analysis by using composites of years with exceptionally high and low summer-sea-ice cover
in the Laptev Sea between June and October. These months coincide with the months we chose for the summer causal-effect
network, but are extended by October to include more of the refreezing phase, which only starts sometime during September.
We select all years which deviate from the mean sea-ice state by more than 1.3 standard deviations. We selected 1.3 standard
deviations as a threshold to a) only use years with significant (larger than one standard deviation) anomalies in sea-ice cover;

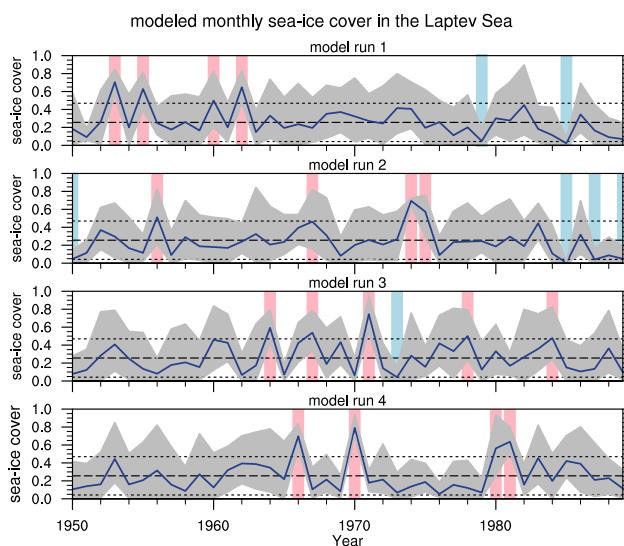


Figure 4. Monthly mean sea-ice cover in the Laptev Sea from June to October in each year. Blue line: mean sea-ice cover over summer period. Grey area: range between minima and maxima of June to October monthly-mean cover. Middle dashed line: average sea-ice cover over all June-to-October means in all years and all model runs, upper/lower dashed line: threshold for composite members (mean plus/minus 1.3 standard deviation), blue/red vertical lines mark composite members for low/high sea-ice cover.

110 and b) to even out number of years contributing to the two composites as well as possible. With 1.3 standard deviations we get 17 years with high sea-ice cover and 7 with low, see Fig. 4.

3 Results

As our main focus lies on the interaction between sea ice and land, we start our analysis by looking at the summer months. The sea ice variability is largest in summer. Afterwards we will cover spring and fall, to find drivers of the melt onset and the
115 refreezing of ice.

3.1 Summer

To understand how sea-ice cover influences the adjacent land, we first look at causal-effect networks during the summer months. Here, both on monthly and on daily scale, we only consider the atmosphere over land, not over the ocean. In this way, direct interactions between sea surface and the atmosphere are excluded. In Fig. 5(A), we see the results using monthly
120 means throughout the summer months of the causal-effect networks analysis. Links with a strength below a threshold of 0.2 are neglected as insignificant in our analysis. Out of the 16 variables used in the set-up, four are connected to sea-ice cover. The strength of the links to sea ice is weak (average strength: 0.25): The (solely contemporary) connections the variables have between each other are much stronger (mean strength: 0.57). For clarity, these connection are not shown in the figure. There

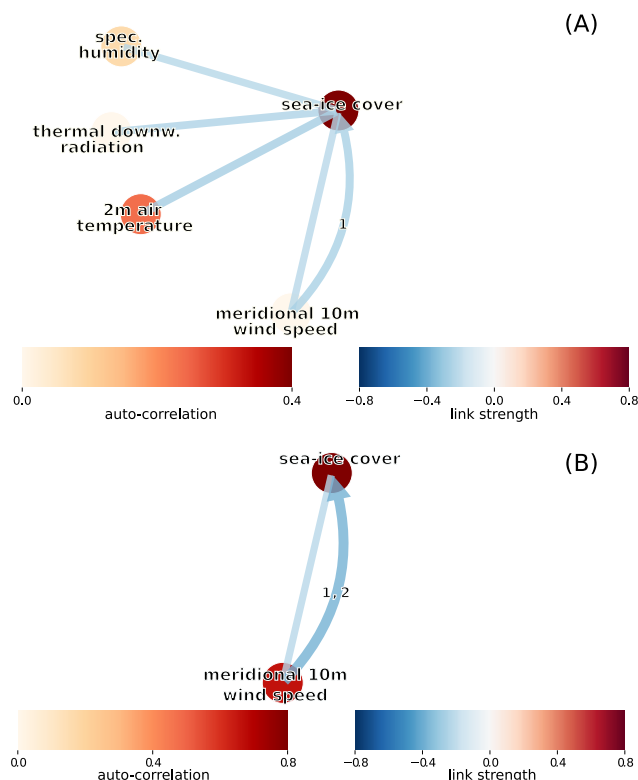


Figure 5. Causal-effect networks using atmospheric time series integrated over the land for summer based on monthly means (A) and daily means (B). Figure includes only those variables which have a significant connection to sea-ice cover. The Color of nodes indicates auto-correlation. Straight lines show contemporaneous links, arrows show causal links with the time lag indexed on the arrow. The color of the arrows represents sign and strength of the link. Blue means that more of one variable coincides with less of the other, whereas red means that changes in the connected variables have the same sign. The link is stronger the darker the color. Variables with significant links to sea-ice cover are specific humidity (spec. humidity) averaged over vertical column, two-meter air temperature (2 m air temperature), meridional ten-meter wind speed (meridional 10 m wind speed) and thermal downward radiation at the surface (thermal downw. radiation).

Table 1. Minimal and maximal values for atmospheric meridional heat (T_v) and moisture (Q_v) transport along a transect at 70N. Values were divided by the mean of each grid cell. Distributions of values for both variables displayed as boxplot in Fig. 6

sea ice	T_v		Q_v	
	min	max	min	max
low cover	-67.7	63.8	-21.97	29.3
mean cover	-90.6	90.4	-31.7	58.3
high cover	-87.5	69.0	-25.6	37.7

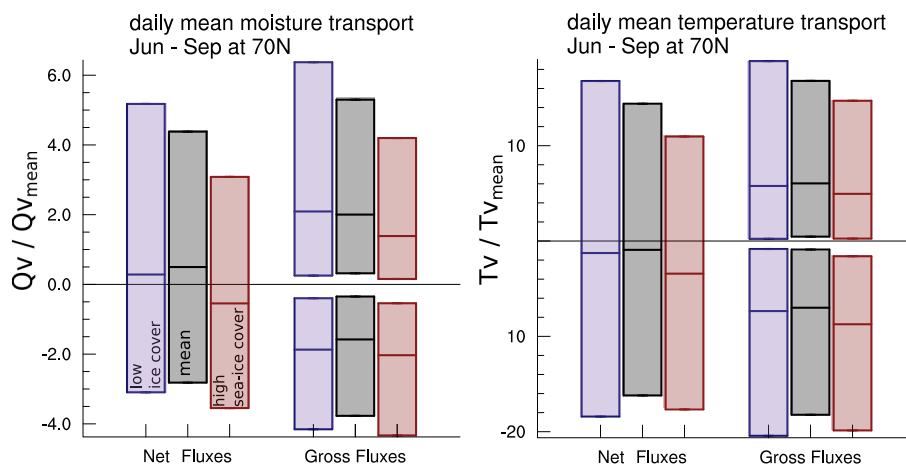


Figure 6. Meridional heat (T_v) and moisture (Q_v) fluxes through a transect at the southern border of the area of interest (70°N). Fluxes were divided by the mean flow through each grid cell over all years. In purple low-sea-ice-cover years are shown, in grey all years and in red high-sea-ice-cover years. 70°N lies just South the coastline on land. We divide the fluxes into net (spatial mean over all data-points at the 70°N edge) and gross (spatial mean over all positive/negative data-points at 70°N boundary). Indicated are the median (centre bar) as well as the first and third quantile of the distribution. For minima and maxima, see Tab. 1.

is only one causal link, from meridional wind speed to sea-ice cover, while all other links are contemporary. All these links
 125 have a negative sign: higher sea-ice cover is associated with a decrease in specific humidity, thermal downward radiation at the surface, 2 m air temperature and 10 m meridional wind speed. Sea-ice cover has less links on daily scale (see Fig. 5(B)) than on the monthly scale. It only links with meridional wind speed, and the only causal link is pointed towards, not away from sea-ice cover, meaning that sea-ice cover is the driven variable.

If we investigate wind with the composites by looking at mean wind-speeds over the Laptev Sea region, we see that wind
 130 direction is variable during the summer months, though there is a slight excess of southward wind. While in the mean about 56% of the days during June to September show winds pointing southward, it is about 53% in the low-sea-ice-cover years and 64% in the high-sea-ice-cover years: High sea-ice cover coincides with a higher fraction of southward wind and vice versa for low sea-ice cover. More precisely, for high-sea-ice-cover years southward transport of moisture and heat is enhanced (see Fig. 6 and Tab. 1). The median of the net flux is lower compared to the mean and this southward shift even leads to a change in
 135 sign for moisture transport from net-northerly to net-southerly transport compared to the mean. For low-sea-ice-cover years on the other hand, both north- and southward transport of moisture and heat increases. Again the median is lower than the median of all years for net fluxes. This indicates that the bulk of transport also shifts towards more southward transport, but for low sea-ice cover, there is a higher spread in the distribution, visible in both the net as well as in the gross fluxes. Using a two-sample Kolmogorov-Smirnov test we find that for both moisture and heat transport the high-sea-ice-cover and low-sea-
 140 ice-cover distributions are significantly different (p -values < 0.001).



3.2 Early melt season of sea ice

Looking at monthly drivers of the early melt of sea ice in spring, we find in total ten variables that have links to sea-ice cover (Fig. 7(A)), and the gross of connections is contemporary (nine variables). Two causal links are found, both of them directed towards sea-ice cover, and with a lag-time of one month. The lagged - causal - links are on average weaker than the contemporary ones.

Returning to the contemporary links, the strongest links connect sea-ice cover to meridional wind speed, sea-ice export and meridional moisture transport respectively. On a daily scale (Fig. 7(B)) zonal wind speed and sea-ice export are still two of the three variables with the strongest connection to sea-ice cover. The third strongest connection now is with sea-ice import. These three directional variables also have causal links influencing sea-ice cover with a time lag of one and two days. Two other variables with causal links pointing towards sea-ice cover are the zonal vector components wind speed and moisture transport. Both have a one-day lag to sea-ice cover, and there is no contemporary link between sea-ice cover and either of the two. On a monthly scale, they have neither a contemporary nor a causal link. Links between sea-ice cover and sea-level pressure, surface longwave downward radiation and specific humidity on the other hand are significant on a monthly but not on a daily scale.

Since the strongest connections that sea-ice cover exhibits during early ice melt are connected to meridional transport and wind, we inspect spatial patterns using the composites for sea-level pressure in May (Fig. 8): We generally have a high over Greenland, but it is stronger for high sea-ice cover than for other years. For high sea-ice cover, we also observe a more distinct polar high, as opposed to low sea-ice cover, when we have a strong high-pressure zone centered over the Chukchi Sea as well as a low over the Kara Sea. Locally over the Laptev Sea, these differences on the large scale lead to contrasting pressure fields. As air flows around pressure systems, we also have vastly different wind patterns in our area of interest. For high sea-ice cover, wind in the Laptev Sea predominantly blows from northeast, carrying air from similar or higher latitudes. For low sea-ice cover on the other hand, we have strong transpolar wind caused by the bipolar pressure field. Consequently, we also have a pronounced transpolar drift of sea ice originating roughly in the Laptev Sea and pointing towards Greenland. Over the Laptev Sea, the average wind direction is northward for low sea-ice cover, and the air masses arrive from southeast, thus carrying comparably warmer air. In the monthly ice-melt causal-effect network (Fig. 7(A)), this warm air is reflected in a contemporary link between air temperature and sea-ice cover.

3.3 Refreezing of the sea in fall

This link is also present during refreeze, when this link is the strongest link of sea-ice cover to any variable (Fig. 7(C)). During ice refreeze the links from sea-ice cover to sea-ice im- and export as well as meridional wind speed are weaker than during the melt onset. Heat and moisture transport do not have significant links to sea-ice cover. The autocorrelation of sea-ice cover, on the other hand, increased from 0.39 to 0.49. The auto-links of air temperature (strength: 0.40) and snow height (strength: 0.53) are also exceptionally strong compared to the other displayed variables. The total number of variables significantly connected to sea-ice cover decreases. The number drops from ten during ice melt to eight during refreeze. Apart from meridional heat and moisture transport, sensible surface heat flux and sea-level pressure disappear to be replaced by snow height and latent surface



175 heat flux. Both of these two variables have only causal and no contemporary links to sea-ice cover. Latent surface heat flux on
the other hand is a dependent variable, with a time lag of three month. The lower sea-ice cover is, the higher are the absolute
fluxes from ocean to atmosphere. The dependency of sea-ice export on sea-ice cover also changes. The contemporary and the
causal link from sea-ice export to sea-ice cover during ice melt is replaced by a causal link from sea-ice cover to sea-ice export
- more sea-ice cover leads to more export in the next month. In general, the number of causal links increases in the ice refreeze
monthly-mean causal-effect network compared to melt. In addition, during refreeze sea-ice cover is also a preceding variable -
180 during melt sea-ice cover is always the influenced variable.

4 Discussion

4.1 Drivers of sea-ice cover

Tracing influences of sea-ice cover on the atmosphere over land with causal-effect networks is not straightforward: sea-ice cover
couples more strongly to atmospheric variables integrated over both land and ocean (Fig. 7(A),(C)) than to the atmosphere over
185 land (Fig. 5). For summer months, where we look solely at the atmosphere over land, we detect no causal link from sea-ice
cover to any variable. The contemporary links that sea-ice cover has are weaker and smaller in number than in the causal-effect
networks of melt and refreeze where we included the atmosphere over the ocean as well: Sea ice seems to have a stronger
impact on the atmosphere directly over the ocean.

A causal link we still observe is from meridional wind speed to sea-ice cover. Moreover, meridional wind speed is the only
190 variable connected to sea-ice cover in the daily-mean summer causal-effect network. During early melt, we observe the same
dependence of sea-ice cover on meridional wind speed.

In spring, we find a counter-intuitive link from air temperature to sea-ice cover (higher temperatures lead to more sea ice, Fig.
7(A)), which is most likely an artefact of the causal-effect network analysis because of our choice of time series: We include
downward longwave radiation in our analysis which is strongly connected to air temperature. But higher air temperatures
195 coincide also with increased upward longwave radiation, which leads to an energy loss at the surface. This upward longwave
radiation was not included in the causal effect network. We think that within the analysis the positive link from temperature
to sea ice is caused by an overcompensation: The additional energy available at the surface through downward radiation is
subtracted from the influence of air temperature on ice, but the energy radiated upward is not. This only becomes important for
the causal link rather than the contemporary connection, because for causal links we can subtract the influence of downward
200 radiation at the present and prior time steps reinforcing the overcompensation.

Besides the link from air temperature to sea-ice cover, variables connected to the pressure field have the strongest links
to sea-ice cover on both monthly and daily scale. Those include local sea-level pressure, and particularly the north/south
components, like meridional wind speed but also meridional moisture transport and sea-ice export. These variables are all
strongly interconnected with each other on the monthly scale (Fig. 7(A)). While the variables have only contemporary links
205 to sea-ice cover on monthly scale, they are driving sea-ice cover with a lag of one to two days in the daily-mean causal-effect
network (Fig. 7(B)). This is in line with a prior observation-based study from Krumpfen et al. (2013), where sea-ice export



from February to May has been singled out as one driver of sea-ice cover. The main local variable determining sea-ice cover in the Laptev Sea during early melt is thus meridional wind, which is also one main driver of sea-ice export. The stronger the northward flow the less sea-ice cover. We can support this with our findings in the May composites (Fig. 8): For high-sea-ice-
210 cover years, wind blows from the northeast carrying colder, less humid air, and, for low-sea-ice-cover years, winds are blowing from southeast enhancing transpolar wind and sea-ice export and bringing warmer humid air. (Meridional) wind depends on air pressure. The large-scale patterns of the May pressure field resemble the patterns of previous mostly observational or reanalysis-based studies (Jaiser et al., 2012; Overland et al., 2012; Wang et al., 2009, e.g.). For high sea-ice cover, sea-level pressure patterns resemble the negative phase of the Arctic Oscillation index (AO) - a high over the central Arctic Ocean (Wang
215 et al., 2009). Additionally, we observe a pronounced high over Greenland. This might hint to Greenland blocking, an event which has been linked to a negative North Atlantic Oscillation index (NAO) (thus also a negative AO). Greenland blocking has been found to cause strong melt of the Greenland ice sheet (Overland et al., 2012) as well as an enhanced influx of moisture in the North Atlantic Region (Yang and Magnusdottir, 2017). This influx then enhances the water-vapour feedback. Instead of a positive AO pattern, low-sea-ice-cover years match an Arctic Dipole (AD) pattern (Fig. 8, similar to Overland et al. (2012);
220 Wang et al. (2009)): We observe a high over the Chukchi and Beaufort Seas with even significantly higher pressure south of the Chukchi Sea and a low over the Barents Sea. The occurrence of the AD pattern fits well with the causal-effect-network-based result, that meridional wind is strongly connected to sea-ice cover in the Laptev Sea. We have pronounced sea-ice export because the AD pattern leads to anomalies in the meridional wind and a stronger transpolar drift of sea ice, while the AO is more connected to zonal wind promoting either convergence or divergence of sea ice in the Arctic (Wang et al., 2009). Advection of
225 Siberian air masses has been observed to link to extremely low sea-ice cover in the Laptev Sea before, for example by Haas and Eicken (2001). Apart from enhanced ice drift, they stress the importance of atmospheric heat content carried into the Laptev Sea. Additionally, temperature fluctuations caused by advection have been identified as a dominant driver of sea-ice variability by Olonscheck et al. (2019). This agrees well with our findings, since, during melt, meridional wind, air temperature as well as meridional heat transport all have strong links to sea-ice cover. Contrasting, we find that the moisture content of the air
230 transported into the Laptev region plays a comparably large role than the heat content of the air. This is in agreement with a satellite- and reanalysis based study by Yang and Magnusdottir (2017) who find that influxes of humid air into high latitudes from the North Atlantic lead to extremely low sea-ice cover in the Greenland, Barents and Kara Seas.

We conclude that during the melt phase, large-scale circulation systems exert a strong influence on the evolution of sea-ice cover. Since melting continues through summer (Kim et al., 2016) until September, the prevailing link from meridional wind
235 speed to sea-ice cover portrays this connection.

During refreeze in fall, meridional wind speed is still important (Fig. 7(B)), but loses its dominance. While the connection between meridional wind speed in the monthly-mean causal-effect network for summer is on the same magnitude as the other connections of sea-ice cover, meridional wind speed is the weakest connection to sea ice during refreeze. Instead, state variables connected to feedback mechanisms, like ice-albedo feedback and water-vapour feedback, are increasingly important and also
240 strongly interconnected. These feedback mechanisms we can already identify during early melt, even though they are less dominant then. In the fall monthly-mean causal effect network (Fig. 7(C)), we observe a cluster of specific humidity, downward



longwave surface radiation and air temperature. Additionally, the auto-correlation of sea-ice cover and air temperature rises. Since the strongest connection between air temperature and sea-ice cover is contemporary and the autocorrelation reaches back one time step, this can be interpreted as part of the strong interdependence of these variables. Sea-ice cover (increase) is also driving both latent surface heat flux and sea-ice export, in contrast to ice melt, when sensible heat fluxes and sea-ice export are driving sea ice (loss). The transition from mainly circulation- to mainly feedback-driven sea-ice cover is in agreement with Barton and Veron (2012) who found moisture-related feedback mechanisms to be a strong driver of Laptev sea ice in September and October. They also reflect the findings of Rigor et al. (2002): During refreeze, the ocean has to emit heat until it is cool enough to freeze, and this emission is reflected in increases in temperature and specific humidity above the water column.

250 4.2 Influence of sea-ice cover on the atmosphere over land

What does this mean for the connection from sea-ice cover to the atmosphere over land? In summer we observe a contemporary connection between sea-ice cover and specific humidity over land (Fig. 5). This link is also present in the ice-melt and refreeze monthly-mean causal effect networks, where we consider the atmosphere over land and ocean. To better understand this connection, we inspect the composites. For high-sea-ice-cover years, we observe more days with on average southward wind - this is in compliance with our earlier findings: Ice export is minimized, and wind tends to carry colder air into the Laptev region. More southward wind also means more southward transport of heat and moisture (Fig. 6 and Tab. 1). When open water areas are reduced compared to the mean state, and both humidity and temperature over the ocean are also reduced, so gross southward transport of both moisture and heat increases just because there is more air flowing south. At the same time, gross northward transport decreases. For low-sea-ice-cover years, there are fewer days with southward wind than usual. Still, we have a higher gross southward transport of heat and moisture because the air is warmer and moister over open water. More heat and moisture gets transported per air volume. In contrast to high-sea-ice-cover years, we also have an increase of transport northward corresponding to our earlier findings: Low-sea-ice-cover years are caused by above average northward wind and an influx of warm and moist air from south. If we compute net moisture and heat fluxes for the low-sea-ice-cover years, the median is only marginally shifted towards an increase of southward transport for both variables. It is remarkable that the increase in southward transport more than balances the increase in northward transport we already identified above as the primary cause of above-average sea-ice cover decrease. We conclude that the contemporary links in the monthly-mean summer causal-effect network incorporate causality in both directions: A decrease in sea-ice cover, as in the ice melt period, is most likely initiated by increased meridional wind pointing north. But the increases in temperature and moisture over land which then accompany low sea ice are both cause, when transported northward, and result of the diminished ice cover, due to consequently enhanced southward transport of heat and moisture in air. This is in line with a model study by Lawrence et al. (2008) who find that rapid sea-ice loss leads to warming on land. In contrast to their analysis, we break down this connection from sea ice to land and identify the responsible atmospheric variables. On the spatial (Laptev Sea) and temporal (days to months) scales analyzed here, we do not find a connection via large-scale circulation starting with changes in sea ice. However, we do not rule out that changes in whole-Arctic sea-ice cover can have an impact on land through large-scale circulation, and connections between sea ice and atmospheric circulation patterns have been shown before (e.g. Ogi et al. (2016)). In contrast to Lawrence et al.



(2008), who focused on the impact of rapid sea-ice loss, without analyzing its drivers, we investigate drivers and impacts of equilibrium sea-ice variability. We find, that over land the impact of sea ice is smaller than the impact of large-scale drivers, which simultaneously lead to changes local sea-ice cover.

5 Conclusions

280 Concerning our research question on the drivers of the sea-ice variability, we conclude from our above model analysis:

- Drivers of sea-ice-cover variability differ during the early melt (April – June) and refreeze (September – November) period. During early melt meridional wind and connected directional variables, like ice-export, are the prime drivers, all of them determined by the large-scale circulation. We find that high sea-ice cover often coincides with an negative Arctic-oscillation pattern, while low sea-ice cover coincides with an Arctic-dipole-like pressure pattern. During refreeze, on the other hand, thermodynamic feedback mechanisms related to temperature and moisture determine the speed of ice formation.

Regarding the connection between sea ice and the state of the atmosphere over land, we find:

- Sea-ice cover is primarily connected to the atmosphere directly above it and signals wash out quickly as we move to the land. Nevertheless, during low-sea-ice-cover years southward heat and especially moisture transport is enhanced. Heat and moisture are both variables which have a strong influence on the carbon budget as they affect both photosynthesis and respiration.
- We show that the impact of sea ice on moisture is at least as strong as on temperature. Studies which only focus on temperature overlook an important pathway of information, especially since the coupling is weak.

A possible explanation for the lack of causal links between atmosphere over land and sea-ice cover lies within temporal scales: The daily variations in the signal emitted by sea-ice cover have a significantly smaller impact than other forcings on the atmosphere over land. Otherwise, we would detect links on a daily scale. A potential slow but persistent forcing from sea-ice cover on the other hand might be diluted on a monthly scale due to the fast interactions within the atmosphere, especially because sea-ice cover exerts a remote forcing. We might still detect a link for the slow forcing, but most likely to several atmospheric variables and a contemporary instead of a causal link.

300 The above analysis was done using the climate of the last century, before the onset of strong changes in the Arctic. The observed loss of sea ice in the Arctic as a whole has been projected to lead to changes in the general circulation pattern, namely via a shift to more negative Arctic Oscillation and North-Atlantic Oscillation indices, which favour high sea-ice cover and thus exert a negative feedback (Jaiser et al., 2012). No clear connection to anthropogenic forcing has been drawn yet for the Arctic Dipole, but from reanalysis we know that there is a higher persistence of this pattern in the 21st century compared to the last 305 (Overland and Wang, 2010). Depending on which of these two shifts persists over the other we can expected a faster or slower decrease of sea ice in the Laptev Sea.



Since sea ice is generally decreasing, we expect that southward heat and moisture transport from the open ocean to the land will increase. Higher temperatures lead to deeper thawing of the seasonally frozen soil layers during summer due to enhanced southward transport of heat and moisture in air. This increases soil-organic-matter decomposition in the then-unfrozen soils, enhancing greenhouse gas emissions, but temperature is also one of the parameters steering the rate of photosynthesis, to name two of many processes which will be altered. Higher air moisture improves photosynthetic rates (high moisture leads to more efficient carbon fixation), changes the amount of (both short- and longwave) incoming solar radiation due to stronger reflection or, if higher humidity in the air leads to higher precipitation and water tables, the pathway of soil-organic-matter decomposition (Shaver et al., 2000).

A general warming and an enhanced hydrological cycle are key features of global climate change (Stocker et al., 2013; Huntington, 2006), and we have shown that the decrease of Laptev Sea sea ice will add to the strength of this general warming and enhanced hydrological cycle over adjacent landmasses. But, as the connection of sea-ice cover to the atmosphere over land is weak, we conclude that future changes on Arctic landscapes and sea-ice loss are mainly driven by large-scale circulation. Though a general decrease of sea ice in the whole Arctic has an effect on large-scale circulation (Li and Wang, 2013; Jaiser et al., 2012) which then effects the Arctic landmasses, the local and direct link from sea-ice cover to adjacent landmasses appears marginal.

Code and data availability. Primary data and scripts used in this study are archived by the Max Planck Institute for Meteorology and can be obtained by contacting publications@mpimet.mpg.de. The model output is available through Niederdrenk and Mikolajewicz (2014) at https://cera-www.dkrz.de/WDCC/ui/cersearch/entry?acronym=DKRZ_LTA_899_ds00003

Author contributions. All authors designed the study together, ZR conducted the data analysis and prepared the manuscript, ALN provided the model simulations and edited the manuscript.

Competing interests. The authors declare no competing interests.

Acknowledgements. We thank Thomas Kleinen for his helpful comments on the manuscript. This work was partially funded by the Max Planck Society.



330 References

- Bareiss, J. and Gørgen, K.: Spatial and temporal variability of sea ice in the Laptev Sea: Analyses and review of satellite passive-microwave data and model results, 1979 to 2002, *Global and Planetary Change*, 48, 28–54, 2005.
- Barton, N. P. and Veron, D. E.: Response of clouds and surface energy fluxes to changes in sea-ice cover over the Laptev Sea (Arctic Ocean), *Climate Research*, 54, 69–84, 2012.
- 335 Bauer, M., Schröder, D., Heinemann, G., Willmes, S., and Ebner, L.: Quantifying polynya ice production in the Laptev Sea with the COSMO model, *Polar Research*, 32, 20922, 2013.
- Deser, C., Walsh, J. E., and Timlin, M. S.: Arctic sea ice variability in the context of recent atmospheric circulation trends, *Journal of Climate*, 13, 617–633, 2000.
- Francis, J. A. and Hunter, E.: Changes in the fabric of the Arctic’s greenhouse blanket, *Environmental Research Letters*, 2, 045011, 2007.
- 340 Graversen, R. G., Langen, P. L., and Mauritsen, T.: Polar Amplification in CCSM4: Contributions from the Lapse Rate and Surface Albedo Feedbacks, *Journal of Climate*, 27, 4433–4450, 2014.
- Haas, C. and Eicken, H.: Interannual variability of summer sea ice thickness in the Siberian and central Arctic under different atmospheric circulation regimes, *Journal of Geophysical Research: Oceans*, 106, 4449–4462, 2001.
- Huntington, T. G.: Evidence for intensification of the global water cycle: Review and synthesis, *Journal of Hydrology*, 319, 83–95, 2006.
- 345 Jacob, D.: A note to the simulation of the annual and inter-annual variability of the water budget over the Baltic Sea drainage basin, *Meteorology and Atmospheric Physics*, 77, 61–73, 2001.
- Jacob, D. and Podzun, R.: Sensitivity studies with the regional climate model REMO, *Meteorol. Atmos. Phys.*, 63, 119–129, <https://doi.org/https://doi.org/10.1007/BF01025368>, 1997.
- Jaiser, R., Dethloff, K., Handorf, D., Rinke, A., and Cohen, J.: Impact of sea ice cover changes on the Northern Hemisphere atmospheric winter circulation, *Tellus Series A - Dynamic Meteorology and Oceanography*, 64, 11 595, 2012.
- 350 Jungclaus, J. H., Fischer, N., Haak, H., Lohmann, K., Marotzke, J., Matei, D., Mikolajewicz, U., Notz, D., and von Storch, J. S.: Characteristics of the ocean simulations in the Max Planck Institute Ocean Model (MPIOM) the ocean component of the MPI-Earth system model, *Journal of Advances in Modeling Earth Systems*, 5, 422–446, <https://doi.org/https://doi.org/10.1002/jame.20023>, 2013.
- Kim, K. Y., Hamlington, B. D., Na, H., and Kim, J.: Mechanism of seasonal Arctic sea ice evolution and Arctic amplification, *Cryosphere*, 10, 2191–2202, 2016.
- 355 Kretschmer, M., Coumou, D., Donges, J. F., and Runge, J.: Using Causal Effect Networks to Analyze Different Arctic Drivers of Midlatitude Winter Circulation, *Journal of Climate*, 29, 4069–4081, 2016.
- Krumpen, T., Janout, M., Hodges, K. I., Gerdes, R., Girard-Ardhuin, F., Holemann, J. A., and Willmes, S.: Variability and trends in Laptev Sea ice outflow between 1992–2011, *Cryosphere*, 7, 349–363, 2013.
- 360 Lawrence, D. M., Slater, A. G., Tomas, R. A., Holland, M. M., and Deser, C.: Accelerated Arctic land warming and permafrost degradation during rapid sea ice loss, *Geophysical Research Letters*, 35, 2008.
- Li, F. and Wang, H. J.: Autumn Sea Ice Cover, Winter Northern Hemisphere Annular Mode, and Winter Precipitation in Eurasia, *Journal of Climate*, 26, 3968–3981, 2013.
- Niederrenk, A. L., Kaleschke, L., and Mikolajewicz, U.: The Arctic hydrologic cycle and its variability in a regional coupled climate model, 365 Phd thesis, 2013.



- Niederrenk, A. L., Sein, D. V., and Mikolajewicz, U.: Interannual variability of the Arctic freshwater cycle in the second half of the twentieth century in a regionally coupled climate model, *Climate Dynamics*, 47, 3883–3900, 2016.
- Niederrenk, L. and Mikolajewicz, U.: Wechselwirkungen zwischen verschiedenen Komponenten des arktischen Klimasystems (bm0899), http://cera-www.dkrz.de/WDC/Compact.jsp?acronym=DKRZ_lta_899, 2014.
- 370 Ogi, M., Rysgaard, S., and Barber, D. G.: The influence of winter and summer atmospheric circulation on the variability of temperature and sea ice around Greenland, *Tellus Series A - Dynamic Meteorology and Oceanography*, 68, 14, 2016.
- Olonscheck, D., Mauritsen, T., and Notz, D.: Arctic sea-ice variability is primarily driven by atmospheric temperature fluctuations, *Nature Geoscience*, 12, 430–+, 2019.
- Overland, J. E. and Wang, M. Y.: Large-scale atmospheric circulation changes are associated with the recent loss of Arctic sea ice, *Tellus Series A - Dynamic Meteorology and Oceanography*, 62, 1–9, 2010.
- 375 Overland, J. E., Francis, J. A., Hanna, E., and Wang, M. Y.: The recent shift in early summer Arctic atmospheric circulation, *Geophysical Research Letters*, 39, 6, 2012.
- Parmentier, F. J. W., Zhang, W. X., Mi, Y. J., Zhu, X. D., van Huissteden, J., Hayes, D. J., Zhuang, Q. L., Christensen, T. R., and McGuire, A. D.: Rising methane emissions from northern wetlands associated with sea ice decline, *Geophysical Research Letters*, 42, 7214–7222, 2015.
- 380 Pithan, F., Medeiros, B., and Mauritsen, T.: Mixed-phase clouds cause climate model biases in Arctic wintertime temperature inversions, *Climate Dynamics*, 43, 289–303, 2014.
- Rigor, I. G., Wallace, J. M., and Colony, R. L.: Response of sea ice to the Arctic oscillation, *Journal of Climate*, 15, 2648–2663, 2002.
- Runge, J., Heitzig, J., Marwan, N., and Kurths, J.: Quantifying causal coupling strength: A lag-specific measure for multivariate time series related to transfer entropy, *Physical Review E*, 86, 15, 2012.
- 385 Runge, J., Petoukhov, V., and Kurths, J.: Quantifying the Strength and Delay of Climatic Interactions: The Ambiguities of Cross Correlation and a Novel Measure Based on Graphical Models, *Journal of Climate*, 27, 720–739, 2014.
- Runge, J., Petoukhov, V., Donges, J. F., Hlinka, J., Jajcay, N., Vejmelka, M., Hartman, D., Marwan, N., Palus, M., and Kurths, J.: Identifying causal gateways and mediators in complex spatio-temporal systems, *Nature Communications*, 6, 2015.
- 390 Sein, D. V., Mikolajewicz, U., Groger, M., Fast, I., Cabos, W., Pinto, J. G., Hagemann, S., Semmler, T., Izquierdo, A., and Jacob, D.: Regionally coupled atmosphere-ocean-sea ice-marine biogeochemistry model ROM: 1. Description and validation, *Journal of Advances in Modeling Earth Systems*, 7, 268–304, 2015.
- Shaver, G. R., Canadell, J., Chapin, F. S., Gurevitch, J., Harte, J., Henry, G., Ineson, P., Jonasson, S., Melillo, J., Pitelka, L., and Rustad, L.: Global warming and terrestrial ecosystems: A conceptual framework for analysis, *Bioscience*, 50, 871–882, 2000.
- 395 Stocker, T., Qin, D., Plattner, G.-K., Alexander, L., Allen, S., Bindoff, N., Bréon, F.-M., Church, J., Cubasch, U., Emori, S., Forster, P., Friedlingstein, P., Gillett, N., Gregory, J., Hartmann, D., Jansen, E., Kirtman, B., Knutti, R., Kumar, K. K., Lemke, P., Marotzke, J., Masson-Delmotte, V., Meehl, G., Mokhov, I., Piao, S., Ramaswamy, V., Randall, D., Rhein, M., Rojas, M., Sabine, C., Shindell, D., Talley, L., Vaughan, D., and Xie, S.-P.: Technical Summary, book section Technical Summary, pp. 33–115, Cambridge University Press, Cambridge, United Kingdom and New York, NY, USA, 2013.
- 400 Vaks, A., Mason, A., Breitenbach, S., Kononov, A., Osinzev, A., Rosenshaft, M., Borshevsky, A., Gutareva, O., and Henderson, G.: Palaeoclimate evidence of vulnerable permafrost during times of low sea ice, *Nature*, 577, 221–225, 2020.
- Wang, J., Zhang, J. L., Watanabe, E., Ikeda, M., Mizobata, K., Walsh, J. E., Bai, X. Z., and Wu, B. Y.: Is the Dipole Anomaly a major driver to record lows in Arctic summer sea ice extent?, *Geophysical Research Letters*, 36, 5, 2009.

<https://doi.org/10.5194/tc-2020-60>
Preprint. Discussion started: 10 March 2020
© Author(s) 2020. CC BY 4.0 License.



Yang, W. C. and Magnusdottir, G.: Springtime extreme moisture transport into the Arctic and its impact on sea ice concentration, *Journal of Geophysical Research: Atmospheres*, 122, 5316–5329, 2017.

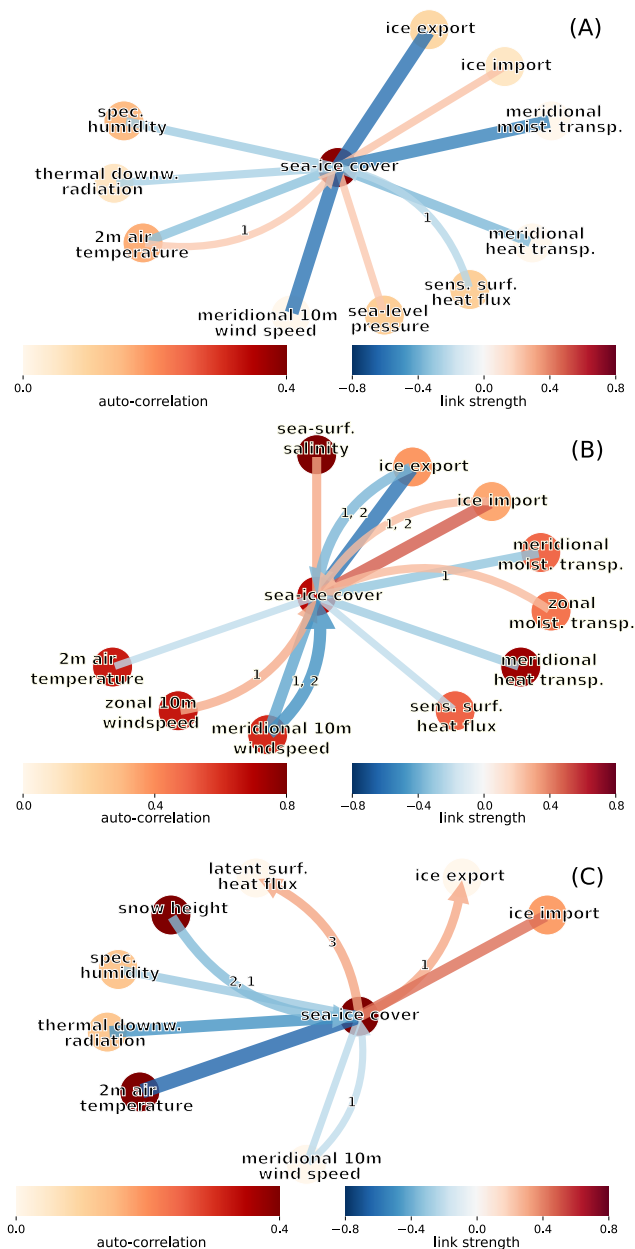


Figure 7. Causal-effect networks considering atmospheric variables over the whole Laptev land and ocean area for ice-melt and ice-refreeze. **(A)** Ice-melt monthly mean. The connection in between the variables (not shown) have a mean strength of 0.44. Contemporary connections between surface longwave downward radiation, air temperature and specific humidity are especially strong (0.77). Same goes for sea-ice im- and export, meridional wind speed, heat and moisture transport (0.626). **(B)** Ice-melt daily means. Similar variables are dominant compared to (A), but more causal links are detected. Note, that the color scale for auto-correlation is different compared to (A) and (C). **(C)** Ice-refreeze monthly mean. Connections between variables (not shown) have a mean strength of 0.44. Contemporary connections between surface longwave downward radiation, air temperature and specific humidity are especially strong (0.79).

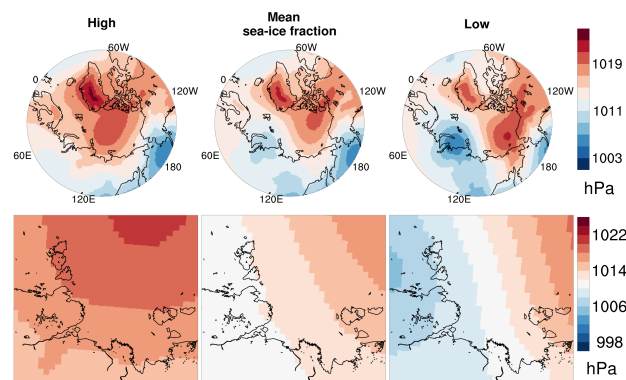


Figure 8. Sea-level air pressure in May on a large scale (upper row) and in the Laptev Sea (lower row). Centre column: May mean of all modelled years; Left/right column: mean over May mean in years of exceptionally high/low sea-ice cover in the Laptev Sea. Dots indicate areas which deviate by at least one standard deviation from the mean state (in the centre column).